Transient juvenile hypoglycemia in GH insensitive Laron syndrome pigs is associated with insulin hypersensitivity

Arne Hinrichs, Kalliopi Pafili, Gencer Sancar, Laeticia Laane, Silja Zettler, Malek Torgeman, Barbara Kessler, Judith Leonie Nono, Sonja Kunz, Birgit Rathkolb, Cristina Barosa, Cornelia Prehn, Alexander Cecil, Simone Renner, Elisabeth Kemter, Sabine Kahl, Julia Szendroedi, Martin Bidlingmaier, John Griffith Jones, Martin Hrabě de Angelis, Michael Roden, Eckhard Wolf

PII: S2212-8778(25)00180-2

DOI: https://doi.org/10.1016/j.molmet.2025.102273

Reference: MOLMET 102273

To appear in: Molecular Metabolism

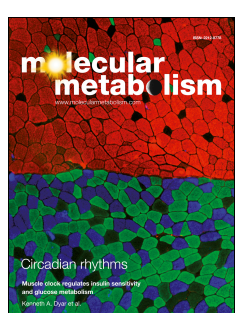
Received Date: 22 May 2025

Revised Date: 2 October 2025 Accepted Date: 12 October 2025

Please cite this article as: Hinrichs A, Pafili K, Sancar G, Laane L, Zettler S, Torgeman M, Kessler B, Nono JL, Kunz S, Rathkolb B, Barosa C, Prehn C, Cecil A, Renner S, Kemter E, Kahl S, Szendroedi J, Bidlingmaier M, Jones JG, Hrabě de Angelis M, Roden M, Wolf E, Transient juvenile hypoglycemia in GH insensitive Laron syndrome pigs is associated with insulin hypersensitivity, *Molecular Metabolism*, https://doi.org/10.1016/j.molmet.2025.102273.

This is a PDF file of an article that has undergone enhancements after acceptance, such as the addition of a cover page and metadata, and formatting for readability, but it is not yet the definitive version of record. This version will undergo additional copyediting, typesetting and review before it is published in its final form, but we are providing this version to give early visibility of the article. Please note that, during the production process, errors may be discovered which could affect the content, and all legal disclaimers that apply to the journal pertain.

© 2025 The Author(s). Published by Elsevier GmbH.



- 1 Transient juvenile hypoglycemia in GH insensitive Laron syndrome pigs is associated
- 2 with insulin hypersensitivity
- 3 Arne Hinrichs^{1,2}, Kalliopi Pafili^{3,4,5}, Gencer Sancar^{5,6,7}, Laeticia Laane^{1,2}, Silja Zettler^{1,2}, Malek
- 4 Torgeman^{1,2}, Barbara Kessler^{1,2}, Judith Leonie Nono^{5,6,7}, Sonja Kunz⁸, Birgit Rathkolb^{1,5,9},
- 5 Cristina Barosa¹⁰, Cornelia Prehn¹¹, Alexander Cecil¹¹, Simone Renner^{1,2,5}, Elisabeth
- 6 Kemter^{1,2,5}, Sabine Kahl^{3,4,5}, Julia Szendroedi^{5,12,13}, Martin Bidlingmaier⁸, John Griffith
- Jones^{10,14}, Martin Hrabě de Angelis^{5,9,15}, Michael Roden^{3,4,5}, Eckhard Wolf^{1,2,5,16}
- 8 ¹ Chair for Molecular Animal Breeding and Biotechnology, Gene Center and Department of
- 9 Veterinary Sciences, LMU Munich, Munich, Germany
- ² Center for Innovative Medical Models (CiMM), LMU Munich, Oberschleissheim, Germany
- ³ Department of Endocrinology and Diabetology, Medical Faculty and University Hospital
- 12 Düsseldorf, Heinrich-Heine-University Düsseldorf, Düsseldorf, Germany
- ⁴ Institute for Clinical Diabetology, German Diabetes Center, Leibniz Center for Diabetes
- 14 Research at Heinrich-Heine-University Düsseldorf, Düsseldorf, Germany
- ⁵ German Center for Diabetes Research (DZD), Neuherberg, Germany
- ⁶ Institute for Diabetes Research and Metabolic Diseases of the Helmholtz Center Munich,
- 17 Tübingen, Germany
- ⁷ Department of Internal Medicine IV, Division of Diabetology, Endocrinology and Nephrology,
- 19 University Hospital of Tübingen, Tübingen, Germany
- 20 8 Endocrine Laboratory, Medizinische Klinik und Poliklinik IV, Klinikum der Universität
- 21 München, Munich, Germany
- ⁹ Institute of Experimental Genetics, German Mouse Clinic (GMC), Helmholtz Center Munich,
- 23 Neuherberg, Germany
- ¹⁰ Center for Neurosciences and Cell Biology, UC Biotech, Cantanhede, Portugal
- ¹¹ Metabolomics and Proteomics Core, Helmholtz Center Munich, Neuherberg, Germany
- ¹² Department of Endocrinology, Diabetology, Metabolism and Clinical Chemistry, Heidelberg
- 27 University Hospital, Heidelberg, Germany
- ¹³ Joint Heidelberg-IDC translational Diabetes Program, Helmholtz Center Munich,
- 29 Neuherberg, Germany
- 30 ¹⁴ Portuguese Diabetes Association, Lisbon, Portugal

Arne Hinrichs (a.hinrichs@gen.vetmed.uni-muenchen.de

31	¹⁵ Chair of Experimental Genetics, School of Life Science Weihenstephan, Technical
32	University Munich, Freising, Germany
33	¹⁶ Interfaculty Center for Endocrine and Cardiovascular Disease Network Modelling and
34	Clinical Transfer (ICONLMU), LMU Munich, Munich, Germany
35	

36

Correspondence:

37	Abstract
38	Background and aims
39	Fasting hypoglycemia has clinical implications for children with growth hormone (GH)-
40	insensitivity syndrome. This study investigates the pathophysiology of juvenile hypoglycemia
41	in a large animal model for GH receptor (GHR) deficiency (the <i>GHR</i> -KO pig) and elucidates
42	mechanisms underlying the transition to normoglycemia in adulthood.
43	Methods
44	Insulin sensitivity was assessed in juvenile and adult GHR-KO pigs and wild-type (WT)
45	controls via hyperinsulinemic-euglycemic clamp (HEC) tests. Glucose turnover was
46	measured using D-[6,6-2H2] glucose and 2H2O. Clinical chemical and targeted metabolomics
47	parameters in blood serum were correlated with qPCR and western blot analyses of liver and
48	adipose tissue.
49	Results
50	GHR-KO pigs showed increased insulin sensitivity (p=0.0019), especially at young age (M-
51	value +34% vs. WT), insignificantly reduced insulin levels, and reduced endogenous glucose $\frac{1}{2}$
52	production (p=0.0007), leading to fasting hypoglycemia with depleted liver glycogen, elevated
53	β-hydroxybutyrate, but no increase in NEFA levels. Low hormone-sensitive lipase
54	phosphorylation in adipose tissue suggested impaired lipolysis in young GHR-KO pigs.
55	Metabolomics indicated enhanced fatty acid beta-oxidation and use of glucogenic amino
56	acids, likely serving as compensatory pathways to maintain energy homeostasis. In
57	adulthood, insulin sensitivity remained elevated but less pronounced (M-value +20%), while
58	insulin levels were significantly reduced, enabling normoglycemia and improved NEFA
59	availability. Increased fat mass, not sex hormones, appeared key to this metabolic transition,
60	as early castration had no effect.
61	Conclusion
62	Juvenile hypoglycemia in GH insensitivity results from excessive insulin sensitivity, reduced
63	glucose production, and impaired lipolysis. Normoglycemia in adulthood emerges through
64	increased adiposity and moderated insulin sensitivity, independently of sex hormones. These
65	findings elucidate the age-dependent metabolic adaptations in GH insensitivity.

69	Keywords
70 71	GH insensitivity; Hypoglycemia; Insulin sensitivity; Large animal model; Glucose metabolism; Beta-oxidation; Metabolomics
72	Highlights:
73 74 75 76 77 78 79	 GHR-KO pigs show transient juvenile hypoglycemia, resembling human Laron syndrome Young GHR-KO pigs display insulin hypersensitivity, reduced EGP, increased beta-oxidation and ketosis Adult GHR-KO pigs accumulate adipose tissue, are less insulin sensitive and normoglycemic The transition to normoglycemia does not depend on sex hormones
80 81 82 83	
84 85	
86	
87 88	
89	
90 91	
92	
93 94	
J -1	

95	Introduction
96 97 98 99	Growth hormone (GH) intrinsically regulates growth and metabolism. Particularly under fasting conditions, elevated GH levels stimulate lipolysis, releasing free fatty acids [1]. Antagonistic effects of GH on insulin action reduce glucose uptake and stimulate endogenous glucose production [2].
100	GH insensitivity due to growth hormone receptor (GHR) deficiency (GHRD, human Laron
101	syndrome, LS) is characterized by postnatal growth retardation and alterations in body
102	composition [3, 4]. LS patients show an increased accumulation of adipose tissue and a
103	reduction in lean/muscle mass. Paradoxically, increased insulin sensitivity despite obesity is
104	described for a cohort of people with LS [5] and is thought to protect against the development
105	of diabetes [6].
106	At infancy, hypoglycemia upon fasting is reported for LS patients and GH-deficient children in
107	general [7] and has clinical implications, leading to heavy sweating, pallor, headache,
108	seizures, and even loss of consciousness [8]. Proposed mechanisms include enhanced
109	insulin sensitivity and impaired endogenous glucose production (EGP), but direct evidence
110	across developmental stages remains limited [9]. The resolution of hypoglycemia in
111	adulthood has been attributed to pubertal changes [7], yet the role of sex hormones in this
112	transition is underexplored and remains unclear. A comprehensive investigation into the age-
113	dependent metabolic adaptations in GHRD is still lacking and essential to understanding GH
114	insensitivity-associated glucose dysregulation.
115	As pigs closely resemble human anatomy, physiology and metabolism in particular [10], we
116	studied the metabolic alterations due to GH insensitivity in a large animal model for Laron
117	syndrome (the GHR-KO pig [11]) in an age-dependent manner. Previous studies already
118	revealed that GHR-KO pigs closely resemble the hallmarks of GH insensitivity such as
119	endocrine disruptions, postnatal growth retardation, altered body composition, juvenile
120	hypoglycemia, decreased insulin secretory capacity, and alterations in metabolic pathways in
121	the liver [11-16]. The current investigations include the assessment of body composition,
122	insulin sensitivity using hyperinsulinemic-euglycemic clamp (HEC) tests, targeted
123	metabolomics, and molecular analyses of liver and adipose tissue. Glucose turnover was
124	assessed with D-[6,6- 2 H $_2$] glucose and 2 H $_2$ O. We investigated age-dependent differences by
125	comparing young, hypoglycemic GHR-KO pigs with adult normoglycemic GHR-KO pigs and
126	age-matched controls as well as adult GHR-KO pigs neutered at young age. We
127	hypothesized that the increased insulin sensitivity is the main driver for fasting hypoglycemia
128	in GH insensitivity, limiting metabolic counter-regulatory mechanisms such as hypoglycemia-
129	induced EGP promotion and lipolysis. Further, we elucidate whether the transition towards
130	normoglycemia at adult age is mediated by sex hormones.

131	Material and Methods
132	Animals and study design
133 134 135 136	All animal procedures were approved by the responsible animal welfare authority (Regierung von Oberbayern; permission ROB 55.2-2532.Vet_02-17-136) and performed according to the German Animal Welfare Act and Directive 2010/63/EU on the protection of animals used for scientific purposes.
137 138 139 140 141 142 143 144 145	In total, 30 pigs were used in the current study. The animals were grouped according to genotype, age, and sex. The collective of young, prepubertal animals contained 5 female <i>GHR</i> -KO and 5 female wild-type (WT) pigs aged 3 months. For the adult age group, 7–8.5 months old pigs were selected because they were sexually mature and <i>GHR</i> -KO pigs exhibit normoglycemia at this stage [11]. The collective of adult animals contained 7 WT pigs (3 males, 4 females) and 7 <i>GHR</i> -KO pigs (3 males, 4 females). Additionally, 3 male and 3 female <i>GHR</i> -KO pigs were neutered at 3 months of age by surgical removal of testes or ovaries. This cohort of early castrated <i>GHR</i> -KO pigs was raised to adult age and compared with the 7 intact <i>GHR</i> -KO pigs.
146 147	GHR-KO pigs carrying a frameshift mutation in GHR exon 3 [11] were propagated by heterozygous × heterozygous mating enabling the comparison to WT littermate controls.
148	Metabolic studies
149 150 151 152 153 154 155 156 157 158 159 160	All animals were equipped with central venous catheters in the internal jugular vein as described previously [17] to maintain constant infusion of tracers, glucose and insulin. Furthermore, the internal carotid artery was catheterized to ensure stress-free withdrawal of repeated blood samples. The surgical procedures were performed one week prior to the experiments. After an overnight fasting period (16 hours), the animals received a priming infusion of 2H_2O (Sigma-Aldrich, St Louis, USA) within 30 minutes to assess the contributions of gluconeogenesis to glucose production from the ratio of the 2H enrichments in carbon 5 over carbon 2 in blood glucose [18-20]. 2H enrichments were measured using LS-MS after derivatization of glucose to acetaminophen glucuronide. The initial dose of 0.5 g 2H_2O per kg body weight was doubled in subsequent experiments and the equilibration time before arterial blood sampling was increased from 3 to 4 hours to achieve an enrichment of 0.5 % 2H_2O in body water.
161 162 163 164	To assess whole-body glucose disposal and endogenous glucose production (EGP), a primed (10 min) infusion of 14 mg/kg/h deuterated glucose (D-[6,6- 2 H $_{2}$]-glucose) was administered beginning with the 2 H $_{2}$ O tracer infusion and maintained with an infusion rate of 2 mg/kg/h until the completion of the clamp procedure [21]. The hyperinsulinemic-euglycemic

165	clamp (HEC) was initiated with a priming insulin dose of 10 mlU per kg body weight per
166	minute (Insuman® Rapid, Sanofi-Aventis, Frankfurt am Main, Germany) for the first 10
167	minutes, followed by a continuous infusion of 1.5 mIU per kg body weight per minute for 3
168	hours [17, 22]. Arterial blood samples were collected at 5-minute intervals for plasma glucose
169	measurement. Simultaneously, an intravenous infusion of 20 % glucose, containing 2.0 %
170	deuterated glucose was adjusted dynamically to maintain a target blood glucose
171	concentration of 90 mg/dL (5 mmol/L). Insulin-stimulated whole-body glucose disposal (M-
172	value) was calculated as previously described during the last 30 minutes of the clamp,
173	including extracellular space correction [23].
174	Endogenous glucose production (EGP) during the hyperinsulinemic-euglycemic clamp (HEC)
175	was fully suppressed in both groups (data not shown). Basal EGP was measured under
176	fasting conditions and was calculated using glucose turnover rates derived from isotope
177	enrichment data applying the Steele's non-steady-state equation [23, 24]. Tracer-derived
178	atom percent enrichment (APE) of deuterated glucose in plasma was measured using gas
179	chromatography-mass spectrometry (GC-MS) [25].
180	Adipose tissue (AT) insulin sensitivity was assessed based on the suppression of non-
181	esterified fatty acid (NEFA) levels. Fasting NEFA levels were measured before insulin
182	infusion, and steady-state NEFA levels were determined during the clamp. NEFA
183	suppression was calculated as: [%] = 100 * (1 – (NEFA _{HEC} / NEFA _{fasting})). Glucose and insulin
184	levels as well as APE of blood glucose during clamp steady state are shown in Figure S1. In
185	addition, tissue-specific insulin resistance was calculated for the basal, fasting state [26]
186	using the following equations:
187	Fasting hepatic insulin resistance (HIR) = EGP $_{fasting}$ [mg/kg*min] * fasting insulin [μ IU/mL]
188	Fasting adipose tissue insulin resistance (AT IR) = plasma NEFA [mmol/L] * fasting insulin
189	[µIU/mL].
190	Metabolite and hormone assays
191	IGF1 concentrations were measured using the iSYS automated chemiluminescent IGF1
192	assay (Immunodiagnostic Systems) as described previously [27]. Commercially available
193	assay kits were applied to measure serum glucagon (10-1281-01, Mercodia), insulin [11], and
194	C peptide (10-1256-01, Mercodia) levels. Plasma was isolated by centrifugation from blood
195	collected in EDTA-coated tubes for the measurement of plasma non-esterified fatty acids
196	(NEFA), triglycerides, cholesterol and β -hydroxybutyrate (BHB; Cayman Chemicals, catalog
197	no: Cay700740) as described previously [28]. Steroid measurements by LC–MS/MS were
198	performed using a commercially available kit (Chromsystems, Darmstadt, Germany)

199	according to the manufacturer's instructions as described previously [29]. Liver glycogen
200	content was measured using a commercial calorimetric kit (ab65620, Abcam). Plasma
201	glycerol levels were measured using the Free Glycerol Reagent (Catalog Number F6428,
202	Sigma-Aldrich) following the manufacturer's instructions.
203	Targeted metabolomics measurements
204	Targeted metabolomics measurements of the pig serum samples were performed using
205	liquid chromatography- and flow injection-electrospray ionization-tandem mass spectrometry
206	(LC- and FIA-ESI-MS/MS) and the Absolute <i>IDQ</i> ™ p180 Kit (BIOCRATES Life Sciences AG,
207	Innsbruck, Austria). The complete assay procedures, sample preparation techniques, and
208	detailed metabolite nomenclature have been previously published [30].
209	Mass spectrometric analyses were done on an API4000 triple quadrupole system (SCIEX
210	Deutschland GmbH, Darmstadt, Germany) equipped with a 1260 Series HPLC (Agilent
211	Technologies Deutschland GmbH, Böblingen, Germany) and an HTC-xc PAL auto sampler
212	(CTC Analytics, Zwingen, Switzerland) controlled by the software Analyst 1.6.2. For the LC-
213	part, compounds were identified and quantified based on scheduled multiple reaction
214	monitoring measurements (sMRM), for the FIA-part on MRM. Data evaluation for
215	quantification of metabolite concentrations and quality assessment were performed with the
216	Web <i>IDQ</i> ™ software package, which is an integral part of the Absolute <i>IDQ</i> ™ kit. Metabolite
217	concentrations were calculated using internal standards and reported in μmol/L (μM).
218	Metabolome data were analyzed using the Metaboanalyst software 6.0 [31]. Values were
219	normalized by sum, data were normalized by log 10 transformation and scaled by Pareto.
220	Necropsy
221	Necropsy was performed after a resting time of 1 week after HEC and an overnight fasting
222	period (16 hours). Pigs were anesthetized by intravenous injection of ketamine (Ursotamin®,
223	Serumwerk Bernburg) and xylazine (Xylazin 2%, Serumwerk Bernburg) followed by fentanyl
224	(Fentadon [®] , Dechra) application. Samples from liver, visceral and subcutaneous adipose
225	tissues were collected subsequent to exsanguination as described previously [32] and
226	immediately frozen on dry ice and stored at -80 °C for molecular profiling. In accordance with
227	a previous study in GHR-KO pigs [11], the ratio of subcutaneous adipose tissue to
228	longissimus lumborum muscle thickness was measured at the level of the last rib.
229	Western blot analysis of phosphoenolpyruvate carboxykinase 1 and hormone sensitive lipase
230	activity
231	Concentrations and phosphorylation states of phosphoenolpyruvate carboxykinase 1 (PCK1)
222	in liver and hormone sensitive linase (HSL) adinose tissues were evaluated by western blot

233 234	intensities were quantified using the ImageJ software package [33].
235	RT-qPCR analysis of candidate transcripts in subcutaneous adipose tissue
236	Frozen subcutaneous adipose tissue samples (100-200 mg) were lysed with 1 mL QIAzol
237	lysis reagent with bead beater in bead tubes (MN, Type F) for 1 min. After adding 250 µL
238	chloroform, tubes were centrifuged at 4 °C at $12,000 \times g$ to collect RNA upper phase.
239	Isopropanol 1:1 in volume was mixed with the supernatant and RNA purification was
240	performed with RNeasy Kit with on column DNase digestion step (Qiagen, catalog no:
241	74106). cDNA was prepared with Transcriptor cDNA Synthesis Kit (Roche, cat no:
242	4897030001) and qPCR was performed with PowerTrack™ SYBR Green Master Mix (Life
243	Technologies, catalog no: A46112). Primers used for qPCR in subcutaneous adipose tissue
244	are listed in Table S1 . The expression pattern was visualized using www.heatmapper.ca [34].
245	Statistical analysis
246	Data were analyzed using PROC GLM (SAS 8.2) taking the effects of genotype (= group;
247	GHR-KO, WT), age (young, adult), and the interaction of group*age into account. Differences
248	between the sexes and the effect of castration in adult GHR-KO pigs were evaluated
249	comparing adult animals using PROC GLM taking the effects of group, sex and the
250	interaction of group*sex into account. Least squares means (LSMs) and standard errors
251	(SEs) of LSMs were calculated for groups and compared using Student t-tests. Correction for
252	multiple testing was performed with the Bonferroni method using the ADJUST = BON
253	statement. Western immunoblot data were evaluated for significant differences between
254	GHR-KO and WT pigs using Mann-Whitney U test. The effects of early castration on sex
255	hormone levels at adult age were evaluated by student`s t test using GraphPad PRISM
256	Version 5.04.
257	Results
258	GHR-KO pigs display juvenile hypoglycaemia, growth retardation and increased
259	accumulation of adipose tissue
260	Fasting blood glucose levels in young <i>GHR</i> -KO pigs were almost halved (-47%) compared to
261	age-matched WT controls (39.5 ± 3.9 mg/dL in <i>GHR</i> -KO vs. 74.5 ± 3.9 mg/dL in WT pigs;
262	p<0.0001, Fig. 1A, Table S2). However, at adult age, fasting glucose levels in <i>GHR</i> -KO pigs
263	were similar to those in adult WT controls (52.1 \pm 3.3 mg/mL in <i>GHR</i> -KO vs. 58.1 \pm 3.3
264	mg/dL in WT pigs; p=0.2099). Serum insulin as well as C-peptide levels were generally lower
265	in GHR-KO pigs (p=0.0005 and p=0.0015 for the effect of group, Fig. 1B, Table S2). The

297	GHR-KO pigs show increased insulin sensitivity, particularly at young age
296	S5).
295	testosterone levels was observed in male adult <i>GHR</i> -KO compared to WT (p<0.0001; Table
294	age (the most relevant parameters are shown in Table S5). A notable increase in
293	hormones, none of the investigated parameters was significantly influenced by sex at adult
292	were similar in early castrated and intact <i>GHR</i> -KO pigs at adult age. Except for sexual
290	p=0.0266), while other clinical-chemical parameters, such as NEFA or BHB (Fig. S3E, F),
290	decreased after castration (14.6 ± 2.7 mg/dL vs. 24.5 ± 2.6 mg/dL in intact <i>GHR</i> -KO pigs;
288	in castrated and intact <i>GHR</i> -KO pigs (Fig. S3C, D). Solely serum triglyceride levels
287 288	compared to intact <i>GHR</i> -KO pigs (p=0.0617; Fig. S3A). Importantly, castration did not prevent normalization of glucose levels at adult age (Fig. S3B). Insulin sensitivity was similar
285 286	Early castration of <i>GHR</i> -KO pigs resulted in diminished sex hormones at adult age (Table S4) and in a mild, insignificant increase in subcutaneous adipose tissue to muscle ratio
284	Sex hormones had no effect on body composition or metabolism of adult GHR-KO pigs
283	(p=0.0042, p=0.1187) but were not affected by group (p=0.9481, p=0.1225).
282	were not affected by genotype nor age. Cortisone and aldosterone levels decreased with age
281	matched WT pigs (p=0.0364; Table S3). Serum corticosterone and deoxycortisone levels
280	Serum cortisol levels were 96% and 21% higher in young and adult GHR-KO vs age-
279	Serum cortisol levels are higher in GHR-KO pigs
278	(p<0.0001, Fig. 1D), while the body composition in WT pigs did not change with age.
277	increased in young and 4.9 times in adult GHR-KO pigs vs. age-matched WT controls
276	subcutaneous adipose tissue to longissimus lumborum muscle height was already 2.7 times
275	accumulated adipose rather than skeletal muscle tissue (see Fig. S2). The ratio of
274	GHR-KO pigs displayed a significantly altered body composition, as they progressively
273	in WT pigs; p<0.0001).
272	reduction of body weight persisted at adult age (48.7 \pm 3.5 kg in <i>GHR</i> -KO vs. 126.2 \pm 3.3 kg
271	age-matched WT controls (18.2 \pm 4.2 kg vs. 45.6 \pm 4.2 kg; p<0.0001, Fig. 1C). This 60%
270	Already at young age, the body weight of GHR-KO pigs was reduced in comparison with
269	compared to age-matched WT controls (p<0.0001, Table 1).
268	Serum IGF1 levels were reduced by 95% in young and by 90% in adult <i>GHR</i> -KO pigs
267	than in the young age group (p=0.1734; Fig 1B).
266	reduction of insulin levels in <i>GHR</i> -KO pigs was more pronounced in the adult (p=0.0001)
266	maduation of insulin levels in OVE KO nine was many property and in the adult (n=0.0004)

- 298 Glucose infusion rate (GIR, **Fig. 2A, B**) during HEC and whole-body insulin sensitivity (M-
- value, mainly representing skeletal muscle insulin sensitivity, Fig. 2C, Table S6) were higher

300 301 302 303 304	in young than in adult animals (WT: +40%; GHR -KO: +57 %; p<0.0001 for the effect of age). GHR -KO pigs exhibited an increased M-value compared with WT pigs (p=0.0019 for the effect of group). This was more pronounced in the juvenile (M value: 32.2 ± 1.6 in GHR -KO vs. 24.1 ± 2.9 mg/kg*min in WT controls; +34%; p=0.0025) than in the adult age group (M value: 20.5 ± 1.4 in GHR -KO vs. 17.2 ± 1.1 mg/kg*min in WT controls; +20%; p=0.1239).
305 306 307	Fasting HIR and AT IR were lower in <i>GHR</i> -KO pigs compared to WT controls (p<0.0001 and p<0.0001 for the effect of group; Fig. 2D,E). NEFA suppression during HEC, representing AT insulin sensitivity, was unaltered in <i>GHR</i> -KO pigs and not affected by age (Table S6).
308 309	Reduced S660 phosphorylation of hormone sensitive lipase, especially in young GHR-KO pigs
310 311 312	As a proxy for hormone sensitive lipase (HSL) activity, we determined its S660 phosphorylation status [35] in both visceral and subcutaneous fat depots. Serine 660 phosphorylation of HSL corelates best with lipolysis activity as shown by mutagenesis
313 314	experiments on rat adipocytes in vitro [36] as well as in human in vivo studies on lipolysis activity in response to stimulation [37]. HSL phosphorylation was decreased in both fat
315	depots of young GHR-KO vs. WT pigs (p<0.01), suggesting reduced activity. In adult GHR-
316	KO pigs, HSL activity was significantly reduced in subcutaneous fat tissue (p<0.05), while
317	only borderline significance (p=0.0571) was found for visceral fat (Fig. 3).
318	Decreased EGP and depleted liver glycogen stores particularly in young GHR-KO pigs
319	Overall, EGP _{fasting} was lower in adult than in juvenile animals (p<0.0001 for the effect of age)
320	and in <i>GHR</i> -KO than in WT pigs (p=0.0007 for the effect of group; Fig 4A, Table S6).
321	This was associated with a complete and partial reduction of liver glycogen stores in young
322	and adult <i>GHR</i> -KO pigs, respectively (Fig. 4B). In the juvenile age group, glycogen content
323	averaged 1.29 \pm 0.4 μ g/mg in WT liver samples, but was consistently below the detection limit
324	(0.4 μg/mg) in <i>GHR</i> -KO liver samples. In the adult group, liver glycogen was detectable in
325	four of seven GHR -KO pigs (0.7 \pm 0.2 μ g/mg), whereas WT animals generally exhibited
326	higher values, with three exceeding the upper detection limit (2.0 μg/mg) and others
327	averaging 1.2±0.6 μg/mg.
328	To determine whether reduced EGP was due to diminished glycogenolysis or
329	gluconeogenesis, we applied the ² H ₂ O tracer method in adult pigs. Sufficient body water
330	enrichment of the ² H ₂ O tracer was achieved in n=3 adult WT, n=5 adult <i>GHR</i> -KO, and n=4
331	young WT pigs, but unfortunately only in n=1 young GHR-KO pig. Analysis of variance did
332	not reveal a significant overall effect for group (p=0.2860; Fig. 4C; Table S6). Within the
333	adult age group, the proportion of gluconeogenesis did not differ significantly between

334 335 336 337 338	genotypes (GHR -KO: 79 ± 9%; WT: 77 ± 18%; Fig. 4C), nor did the absolute rate of gluconeogenesis-derived glucose (1.1 ± 0.2 vs. 1.3 ± 0.2 mg/kg*min; Fig. 4D). Similar glucagon levels (p=0.1463; Table S2) and comparable hepatic expression of phosphoenolpyruvate carboxykinase 1 (PCK1; Fig. 4E) across age and genotype further suggest that gluconeogenic capacity was not impaired.
339	Juvenile hypoglycemia is associated with increased BHB but not NEFA levels
340 341 342 343 344	At young age, fasting BHB levels of <i>GHR</i> -KO pigs were on average 7.2 times higher than in WT controls (16.6 \pm 2.0 vs. 2.3 \pm 0.4 nmol/mL; p<0.0001; Fig. 5A). At adult age, BHB levels of <i>GHR</i> -KO pigs were 3.1 times higher than in age-matched controls (8.5 \pm 0.9 vs. 2.7 \pm 0.3 nmol/mL; p=0.0001), whose values remained relatively constant (p=0.0002 for the interaction of group*age).
345 346 347 348 349 350 351 352 353 354 355 356 357 358 359	Despite hypoglycemia and ketosis, young GHR -KO pigs showed no increase in NEFA levels, which were in fact slightly decreased in comparison with young controls (0.70 \pm 0.07 vs. 0.80 \pm 0.08 mmol/L; p=0.2174; Fig. 5B, Table S2). NEFA levels were generally higher in young animals (p<0.0001 for the effect of age), with a pronounced age-dependent decrease was observed mainly in WT pigs (p=0.0231 for the interaction of group*age). In adult GHR -KO pigs, displaying normoglycemia and less pronounced ketosis, NEFA levels were higher than in adult WT controls (0.50 \pm 0.06 vs. 0.30 \pm 0.06 mmol/L; p=0.0299). Similar trends were observed for glycerol with lower levels in young GHR -KO compared to WT pigs (79.6 \pm 13.1 vs. 135.2 \pm 28.5 μ mol/L; p=0.0290) and no age-related decrease in glycerol levels as observed in WT pigs (p=0.0197 for the interaction of group*age; Fig. 5C, Table S2). Fasting triglyceride levels were as a trend decreased by 35% in young and 24% in adult GHR -KO pigs (p=0.2500 for the effect of group; Fig. 5D; Table S2). Serum levels of cholesterol as well as HDL and VDL cholesterol were similar in GHR -KO and WT pigs and displayed an overall decrease with age (p=0.0105 and p=0.0554 for the effect of age; Table S2).
360	Increased fatty acid beta-oxidation and utilization of glucogenic amino acids in GHR-KO pigs
361 362 363 364 365 366 367	To elucidate metabolic alterations in <i>GHR</i> -KO pigs in greater detail, we analyzed serum samples by targeted metabolomics. Specifically, we aimed to understand how elevated BHB levels can be maintained without a corresponding increase in NEFA concentrations, particularly in young <i>GHR</i> -KO pigs. In total, 187 metabolites, including 39 acylcarnitines, free carnitine, 21 amino acids, 21 biogenic amines, 14 lysophosphatidylcholines, 76 phosphatidylcholines, and 15 sphingolipids, were quantified and physiologically relevant ratios calculated (Tables S7-12). Partial Least Squares Discriminant Analysis (PLS-DA)
368	clearly separated metabolomic profiles from <i>GHR</i> -KO and control samples (Fig. S4)

369	Our results indicate an increased beta-oxidative activity in GHR-KO pigs, as increased
370	concentrations of long-chain (C14-C18), as well as short-chain acylcarnitines (C2-C5) were
371	detected (p=0.0026 and p<0.0001 for the effect of group; Fig. 6A, B), while carnitine (C0;
372	Fig. 6C) levels were unaltered. An increased mitochondrial uptake of NEFAs via the carnitine
373	palmitoyltransferase 1A (CPT1A) in GHR-KO pigs is indicated by an increased ratio of long-
374	chain acylcarnitines (C16 + C18) to free carnitine (C0) (CPT1 ratio; p=0.0097 for the effect of
375	group; Fig. 6D). Overall, the CPT1A activity was higher in young than in adult animals
376	(p<0.0001 for the effect of age). An increased ratio of C2 + C3 acylcarnitines to C0 in GHR-
377	KO pigs (p<0.0001 for the effect of group; Fig. 6E) further indicates an increased beta-
378	oxidation rate [38], degrading NEFAs to acetyl-CoA as a substrate for ketogenesis and
379	explaining the highly elevated BHB levels in young GHR-KO pigs.
380	An increased utilization of amino acids as substrates for gluconeogenesis in GHR-KO pigs is
381	indicated by significantly decreased plasma concentrations of solely glucogenic amino acid
382	(p=0.0001 for the effect of group, Fig. 7A) while levels of solely ketogenic amino acids were
383	increased (p=0.003 for the effect of group, Fig. 7B). Notably, we observed decreased levels
384	of branched chain amino acids (BCAAs, p=0.0344; Table S8) in <i>GHR</i> -KO pigs, which is of
385	particular interest, as increased BCAA levels are considered as risk factor for the
386	development of diabetes [39].
387	The lipid profile of <i>GHR</i> -KO pigs was largely comparable to that of WT controls, as the ratio
388	of unsaturated to saturated lysophosphatidylcholines showed no significant group-related
389	differences (Fig. S5A), and the corresponding ratio for phosphatidylcholines was only mildly
390	elevated in <i>GHR</i> -KO pigs (p=0.0710 for the effect of group; Fig. S5B).
391	Adipose tissue accumulation in GHR-KO pigs without major canonical gene expression
392	alterations
393	Since a previous study in GHR-KO pigs found many gene sets and pathways related to
394	metabolism enriched in the transcriptome of predominantly subcutaneous but not visceral
395	adipose tissue [15], we evaluated the expression pattern of selected genes involved in
396	adipogenesis, lipolysis as well as glucose metabolism, insulin signaling, and inflammation via
397	qPCR in the subcutaneous depot. Remarkably, the expression pattern appeared less
398	different than expected from the obvious degree of obesity in GHR-KO pigs (see Fig. S6,
399	Table S13). The transcript levels of genes involved in lipid and fatty acid synthesis such as
400	PPARG, FASN, SCD, ME1, ACACA and EVOVL6 were not significantly altered in GHR-KO
401	adipose tissue. The unaltered mRNA expression for stearoyl-CoA desaturase (SCD;
402	p=0.9275), an enzyme that introduces a double bond into saturated fatty acids, converting
403	them into monounsaturated fatty acids [40], aligns with lipid profiles assessed for GHR-KO
404	pigs. Higher NPR3 transcript levels in GHR-KO pigs (p<0.0001) are interesting since the

corresponding protein can block some of the lipolytic action usually induced by natriuretic 405 406 peptides [41]. Obesity-related desensitization towards insulin action in adipose tissue is commonly associated with a reduced expression of the INSR [42], which was not the case in 407 408 GHR-KO subcutaneous adipose tissue. Further, the expression of GLUT4, which represents 409 a marker for systemic insulin sensitivity [42], appeared unaltered. While an increased 410 expression of MCP1 (p=0.006) can indicate low-grade inflammation in association with 411 obesity [43], IL6 and IL1B transcript levels were not or only as a trend increased, which 412 appears in line with a protection against obesity-related adipose tissue inflammation observed in Ghr-KO mice [44]. Taken together, our results indicate that the increased 413 accumulation of adipose tissue in GHR-KO pigs does not lead to the common obesity-related 414 415 pathophysiology. **Discussion** 416 417 GHR-KO pigs reflect the phenotype of increased insulin sensitivity despite obesity observed in human LS patients [5]. While the fasting period was similar in all animals, young GHR-KO 418 419 pigs displayed a pronounced negative energy balance potentially due to reduced substrate 420 availability. That includes depleted liver glycogen stores, contributing to reduced hepatic 421 glucose output, juvenile hypoglycemia and increased ketogenesis. Our data further indicates 422 an increased utilization of NEFA for beta-oxidation combined with a decreased NEFA release 423 from adipose tissue lipolysis, both contributing to a lack of increase in circulating NEFA 424 despite elevated BHB levels. Our results of decreased fasting EGP and reduced fasting HIR and AT IR mirror the opposite 425 effects of GH on glucose metabolism assessed in acromegaly. In those patients, GH excess 426 results in a lean but insulin-resistant phenotype (reviewed in [45]). Arlien-Søborg et al. [46] 427 investigated metabolic properties of patients with acromegaly using [3-3H]-glucose tracers in 428 429 combination with hyperinsulinemic-euglycemic clamp studies before and after disease control. Within that study, it was assessed that GH overabundance is associated with 430 431 increased EGP [46, 47]. Also, increased AT IR was present in patients with acromegaly [46] due to the function of GH-mediated NEFA release from adipose tissues (reviewed in [48]). 432 Our study identified increased insulin sensitivity as the major driver of juvenile hypoglycemia 433 in GHR-KO pigs. Hypoglycemia due to increased insulin sensitivity is also reported for 434 human type 2 diabetic patients after treatment with insulin-sensitizing drugs [49, 50] and after 435 gastric bypass surgery [51]. Under physiological conditions, GH provides major counter-436 regulatory responses to hypoglycemia, stimulating lipolysis and inducing insulin resistance 437 (reviewed in [2, 45, 52]). In its absence, GH-insensitive individuals face impaired glucose 438 homeostasis, with fasting hypoglycemia - even below 30 mg/dL - reported in children with 439 Laron syndrome [53]. Resembling that phenotype, young hypoglycemic GHR-KO pigs

440

441	displayed markedly reduced fasting endogenous glucose production and diminished lipolytic
442	activity, resulting in limited NEFA availability. To compensate, these animals shifted toward
443	enhanced ketogenesis, fueled by increased beta-oxidation and acetyl-CoA production,
444	further depleting NEFA reserves. Previous investigations of functional changes in the liver
445	using proteomics and metabolomics revealed alterations in fatty acid and amino acid
446	metabolism related pathways in 6-month-old <i>GHR</i> -KO pigs [54]. This study inter alia detected
447	3-hydroxy-3-methylglutaryl-CoA synthase 2 as the protein with the highest abundance
448	increase in GHR-KO liver samples. As the key enzyme for ketogenesis, it converts acety-
449	CoA and acetoacetyl-CoA into the key intermediate for the synthesis of ketone bodies
450	(reviewed in [55]). The utilization of amino acids as gluconeogenic substrates in GHR-KO
451	pigs corresponds with generally increased levels of proteins especially involved in amino acid
452	catabolism and the TCA cycle in the liver [54] and can contribute to the phenotype of reduced
453	muscle mass in GH insensitivity [11]. Children generally have a higher rate of ketogenesis
454	during fasting [56], implying the functional importance of GH-mediated lipolysis in early life.
455	This is supported by the higher NEFA levels in young compared to adult WT pigs. This
456	physiological higher availability of NEFA at young age is lacking in GHR-KO pigs as well as
457	in patients with GH insensitivity or deficiency, possibly contributing to their metabolic
458	problems at young age.
459	In line with the phenotype of human patients, we observed a normalization of fasting glucose
460	levels in GHR-KO pigs at adult age. To explain this phenomenon in GH-insensitive or
461	deficient patients, several hypotheses have been proposed, including a decrease in insulin
462	sensitivity [53] due to the impact of rising sex hormone concentrations during puberty [7] and
463	an involvement of the increasing accumulation of adipose tissues [57]. In fact, we observed a
464	decrease in insulin sensitivity in adult <i>GHR</i> -KO pigs, compared to their young counterparts.
465	Nevertheless, insulin sensitivity was still increased in comparison with age-matched WT
466	controls. The decrease in insulin sensitivity was accompanied by a decrease in fasting insulin
467	levels in adult GHR-KO pigs. A more pronounced decrease in insulin secretion at adult age
468	has been shown in previous studies in young and adult GHR-KO pigs [16]. A decrease in
469	insulin secretion can serve as a compensatory mechanism on insulin hypersensitivity [58]
470	and lead to normoglycemia at adult age. Conversely, the insulin hypersensitivity in young
471	GHR-KO pigs may also be a consequence of their reduced insulin secretory capacity. A
472	counterregulatory increase in insulin sensitivity is described upon the loss of insulin secretory
473	capacity in hereditary haemochromatosis [59]. The metabolic state in adult GHR-KO pigs can
474	be characterized as less catabolic than in young animals, including the maintenance of
475	normoglycemia and a less pronounced ketosis. The dampened insulin sensitivity in adult
476	GHR-KO pigs allowed a sufficient release of NEFAs from adipose tissues, which
477	accumulated with age.

Puberty is commonly associated with a decrease in insulin sensitivity and a compensatory increase in insulin secretion (reviewed in [9]). This is indeed resembled in WT pigs, in line with previous studies [16]. In some LS patients, it has been observed that the transition to normoglycemia occurred around the age when sexual maturity was attained, but this was not recapitulated in *Ghr*-KO mice (reviewed in [9]). Our present study shows that sex hormones are not causal for the normalization of blood glucose levels in GH insensitivity as early castration of *GHR*-KO pigs did not preserve the hypoglycemic phenotype into adulthood.

The lack of lipolytic GH action drives the accumulation of adipose tissue in GH insensitivity (reviewed in [48]). In *Ghr*-KO mice, a preferential accumulation of subcutaneous adipose tissue is commonly seen in association with improved insulin sensitivity [60] and *Ghr*-KO mice remain insulin sensitive when fed a high-fat diet (reviewed in [4]). Further, adipose tissue from *Ghr*-KO mice even improves insulin sensitivity when transplanted into wild-type mice [61]. A direct comparison of adipose tissue morphology and transcriptome revealed similarities between human LS patients and *GHR*-KO pigs regarding adipocyte size and gene expression profile [15]. Our results show that the increase in adipose tissue in GH insensitivity is not strictly associated with the common obesity-related pathophysiology as a mechanism to promote insulin resistance with age. On the other hand, we observed a decreased HSL activity mainly in young *GHR*-KO pigs, while the trend towards normalization of HSL activity in adult animals was associated with a more sufficient NEFA release upon fasting and dampened insulin sensitivity. It has to be noted, that the activity of HSL has solely been assessed within the distinct age groups while a direct *in vivo* or *ex vivo* estimation of lipolytic activity could help to assess the age-specific activity.

These observations prompt the fundamental question, by what mechanisms the enhanced insulin sensitivity in GH insensitivity is mediated. Previous studies in *GHR*-KO pigs revealed a decreased pancreatic beta-cell volume, which was associated with a decreased insulin secretory capacity [16]. In spite of the generally low insulin levels in GH insensitivity, *GHR*-KO pigs displayed a preserved glucose tolerance as observed in human LS patients [5], most likely due to the markedly increased insulin sensitivity. This effect is likely attributable to both, a direct modulation of insulin signaling pathways, and indirect mechanisms associated with broader metabolic alterations. Evidence from *Ghr*-KO mice indicates an increased expression of hepatic insulin receptors, along with augmented phosphorylation of downstream signaling components [62]. That is seen as a compensatory mechanism to the decreased insulin secretory capacity [16], contributing to an elevated responsiveness to insulin stimulation in the absence of GH signaling (reviewed in [2]). In GHR intact individuals, GH promotes lipolysis and the release of NEFAs, which directly impair insulin sensitivity. The accumulation of lipids in insulin-responsive tissues is considered a key driver of lipid-induced insulin resistance (reviewed in [63]). In particular, the intramyocellular buildup of diacylglycerol (DAG) and

ceramides, NEFA-derived signaling intermediates, has been shown to impair insulin signaling and reduce glucose uptake in skeletal muscle (reviewed in [64, 65]). Further, it has been discussed, that NEFA oxidation suppresses pyruvate dehydrogenase activity, raising intracellular glucose-6-phosphate concentrations, which prevents glucose uptake, contributing to fat-induced insulin resistance by inhibiting insulin-stimulated glucose uptake ([66, 67], reviewed in [64]). In line with that, the transition towards normoglycemia with age appears directly linked to body adipose tissue content in hypopituitary children, and lean GH-deficient children are more prone to show symptomatic hypoglycemia ([57], reviewed in [68]). From this perspective, we propose a dynamic model in which an increased release of NEFAs from accumulating adipose tissue with age triggers a reduction of the exaggerated insulin sensitivity. This may establish a self-reinforcing cycle, decreasing the insulin-mediated suppression of HSL activity and NEFA release observed in adult GHR-KO pigs. Future studies of arteriovenous metabolomics [69] in GHR-KO pigs can directly assess the remodeling of metabolic flux between organs and tissues. This approach can determine to what extent the lack of a corresponding increase in NEFA levels during increased ketogenesis in young GHR-KO pigs is due to increased utilization of free fatty acids or to insufficient release from adipose tissues.

Conclusion

515516

517518

519

520

521

522

523524

525

526

527

528

529530

531

532

540

- This study uncovers insulin sensitivity–driven ketotic hypoglycemia as a core consequence of
- 534 GH insensitivity in young GHR-KO pigs, linked to impaired lipolysis and altered substrate
- 535 utilization during development. The age-dependent restoration of metabolic balance appears
- to be associated with progressive fat mass accumulation, but not with rising sex hormones.
- An adequate NEFA release in adult *GHR*-KO pigs can contribute to a relative decline in
- insulin sensitivity compared to their younger counterparts. Reduced insulin secretion is
- another counterregulatory mechanism to avoid hypoglycemia in adult *GHR*-KO pigs.

Funding

- This study was funded by the Deutsche Forschungsgemeinschaft (DFG, German Research
- 542 Foundation; HI 2206/2-1; FOR 5795; Project number 441815498; 536691227; CRC-TR 127;
- 543 CRC-TR 205), by the German Center for Diabetes Research (DZD; FKZ 82DZD08D03) and
- the Portuguese Foundation for Science and Technology (FCT-FEDER-
- 545 02/SAICT/2017/028147 and UIDB/Multi/04462/2020). Structural funding for the Center for
- Neurosciences and Cell Biology and the UC-NMR facility is supported in part by FEDER –
- 547 European Regional Development Fund through the COMPETE Programme, Centro 2020
- 548 Regional Operational Programme, and the Portuguese Foundation for Science and
- Technology through grants UIDB/04539/2020; UIDP/04539/2020, LA/P/0058/2020 POCI-01-
- 550 0145-FEDER-007440; REEQ/481/QUI/2006, RECI/QEQ-QFI/0168/2012, CENTRO-07-

551	CT62-FEDER-002012, and Rede Nacional de Ressonancia Magnética Nuclear. The
552	research of KP is supported by the Deutsche Forschungsgemeinschaft (DFG, German
553	Research Foundation): Project number 493659010 in the context of the Clinician Scientist
554	Program (FUTURE-4-CSPMM) and by grants from the German Diabetes Research (DZD)
555	foundation and the Heinrich-Heine-University Düsseldorf.
556	Credit authorship contribution statement
557	Arne Hinrichs: Writing – original draft, Investigation, Formal analysis, Data curation,
558	Conceptualization. Kalliopi Pafili: Methodology, Formal Analysis, Writing – review & editing.
559	Gencer Sancar: Investigation, Resources, Methodology, Writing – review & editing. Laeticia
560	Laane: Investigation. Silja Zettler: Investigation. Malek Torgeman: Data curation. Barbara
561	Kessler: Investigation. Judith Leonie Nono: Methodology. Sonja Kunz: Methodology.
562	Birgit Rathkolb: Methodology. Cristina Barosa: Methodology. Cornelia Prehn:
563	Methodology. Alexander Cecil: Data curation. Simone Renner: Investigation, Methodology,
564	Conceptualization. Elisabeth Kemter: Methodology. Sabine Kahl: Methodology. Julia
565	Szendrödi: Conceptualization, Methodology. Martin Bidlingmaier: Methodology. John
566	Griffith Jones: Methodology. Martin Hrabě de Angelis: Methodology. Michael Roden:
567	Writing – review & editing, Supervision, Methodology. Eckhard Wolf: Writing – review &
568	editing, Supervision, Methodology.
569	Declaration of competing interests None
570	Acknowledgements
571	The authors thank David AJ López, Tatiana Schröter, and Sarina Benedix for excellent
572	technical support, and Sylvia Hering and Harald Paul for expert animal management. We
573	thank Julia Scarpa and Silke Becker for supporting the metabolomics measurements
573 574	
	thank Julia Scarpa and Silke Becker for supporting the metabolomics measurements
574	thank Julia Scarpa and Silke Becker for supporting the metabolomics measurements performed at the Helmholtz Zentrum München, Metabolomics and Proteomics Core.
574 575	thank Julia Scarpa and Silke Becker for supporting the metabolomics measurements performed at the Helmholtz Zentrum München, Metabolomics and Proteomics Core. Figure 1. Fasting serum glucose and insulin levels, body weight, and body composition of
574 575 576	thank Julia Scarpa and Silke Becker for supporting the metabolomics measurements performed at the Helmholtz Zentrum München, Metabolomics and Proteomics Core. Figure 1. Fasting serum glucose and insulin levels, body weight, and body composition of young and adult <i>GHR</i> -KO pigs and WT controls. (A) Fasting serum glucose; (B) Fasting
574 575 576 577	thank Julia Scarpa and Silke Becker for supporting the metabolomics measurements performed at the Helmholtz Zentrum München, Metabolomics and Proteomics Core. Figure 1. Fasting serum glucose and insulin levels, body weight, and body composition of young and adult <i>GHR</i> -KO pigs and WT controls. (A) Fasting serum glucose; (B) Fasting serum insulin. (C) Body weight. (D) Fat-to-muscle ratio (thickness of overlaying
574575576577578	thank Julia Scarpa and Silke Becker for supporting the metabolomics measurements performed at the Helmholtz Zentrum München, Metabolomics and Proteomics Core. Figure 1. Fasting serum glucose and insulin levels, body weight, and body composition of young and adult <i>GHR</i> -KO pigs and WT controls. (A) Fasting serum glucose; (B) Fasting serum insulin. (C) Body weight. (D) Fat-to-muscle ratio (thickness of overlaying subcutaneous adipose tissue / longissimus lumborum muscle height). The box plots show
574 575 576 577 578 579	thank Julia Scarpa and Silke Becker for supporting the metabolomics measurements performed at the Helmholtz Zentrum München, Metabolomics and Proteomics Core. Figure 1. Fasting serum glucose and insulin levels, body weight, and body composition of young and adult <i>GHR</i> -KO pigs and WT controls. (A) Fasting serum glucose; (B) Fasting serum insulin. (C) Body weight. (D) Fat-to-muscle ratio (thickness of overlaying subcutaneous adipose tissue / longissimus lumborum muscle height). The box plots show median, interquartile range (box) and extremes (whiskers). The mean is marked as "+".
574 575 576 577 578 579 580	thank Julia Scarpa and Silke Becker for supporting the metabolomics measurements performed at the Helmholtz Zentrum München, Metabolomics and Proteomics Core. Figure 1. Fasting serum glucose and insulin levels, body weight, and body composition of young and adult <i>GHR</i> -KO pigs and WT controls. (A) Fasting serum glucose; (B) Fasting serum insulin. (C) Body weight. (D) Fat-to-muscle ratio (thickness of overlaying subcutaneous adipose tissue / longissimus lumborum muscle height). The box plots show median, interquartile range (box) and extremes (whiskers). The mean is marked as "+". Results of analysis of variance are indicated: G: p-value of the effect of Group; A: p-value of
574 575 576 577 578 579 580 581	thank Julia Scarpa and Silke Becker for supporting the metabolomics measurements performed at the Helmholtz Zentrum München, Metabolomics and Proteomics Core. Figure 1. Fasting serum glucose and insulin levels, body weight, and body composition of young and adult <i>GHR</i> -KO pigs and WT controls. (A) Fasting serum glucose; (B) Fasting serum insulin. (C) Body weight. (D) Fat-to-muscle ratio (thickness of overlaying subcutaneous adipose tissue / longissimus lumborum muscle height). The box plots show median, interquartile range (box) and extremes (whiskers). The mean is marked as "+". Results of analysis of variance are indicated: G: p-value of the effect of Group; A: p-value of the effect of Age; G*A: p-value of the interaction Group*Age. Means with different superscript
574 575 576 577 578 579 580 581 582	thank Julia Scarpa and Silke Becker for supporting the metabolomics measurements performed at the Helmholtz Zentrum München, Metabolomics and Proteomics Core. Figure 1. Fasting serum glucose and insulin levels, body weight, and body composition of young and adult <i>GHR</i> -KO pigs and WT controls. (A) Fasting serum glucose; (B) Fasting serum insulin. (C) Body weight. (D) Fat-to-muscle ratio (thickness of overlaying subcutaneous adipose tissue / longissimus lumborum muscle height). The box plots show median, interquartile range (box) and extremes (whiskers). The mean is marked as "+". Results of analysis of variance are indicated: G: p-value of the effect of Group; A: p-value of the effect of Age; G*A: p-value of the interaction Group*Age. Means with different superscript letters are significantly different (p<0.05).

586 587 588 589	interquartile range (box) and extremes (whiskers). The mean is marked as "+". Results of analysis of variance are indicated: G: p-value of the effect of Group; A: p-value of the effect of Age; G*A: p-value of the interaction Group*Age. Means with different superscript letters are significantly different (p<0.05).
590 591	Figure 3. Western blot analysis of hormone sensitive lipase (HSL) S660 phosphorylation in subcutaneous (A) and visceral (B) adipose tissue. Significant differences in the ratio of
592	phosphorylated to total HSL (pHSL/HSL) are indicated by asterisks. *p < 0.05; **p < 0.01.
593	Figure 4. Endogenous glucose production in GHR-KO pigs and WT controls. (A) Fasting
594	endogenous glucose production. (B) Liver glycogen content. (C) Contribution of
595	gluconeogenesis to EGP. (\mathbf{D}) glucose from gluconeogenesis determined by the 2H_2O
596	approach (numbers of animals assessed within the distinct group are indicated by the
597	corresponding dots). (E) Western blot analysis of phosphoenolpyruvate carboxykinase 1
598	(PCK1) abundance in liver samples from young and adult WT and GHR-KO pigs. The box
599	plots show median, interquartile range (box) and extremes (whiskers). The mean is marked
600	as "+". Results of analysis of variance are indicated: G: p-value of the effect of Group; A: p-
601	value of the effect of Age; G*A: p-value of the interaction Group*Age. Means with different
602	superscript letters are significantly different (p<0.05).
603	Figure 5. Fasting serum levels of (A) β -hydroxybutyrate, (B) non-esterified fatty acids
604	(NEFA), (C) glycerol, and (D) triglycerides in young and adult GHR-KO pigs and WT controls.
605	The box plots show median, interquartile range (box) and extremes (whiskers). The mean is
606	marked as "+". Results of analysis of variance are indicated: G: p-value of the effect of
607	Group; A: p-value of the effect of Age; G*A: p-value of the interaction Group*Age. Means with
608	different superscript letters are significantly different (p<0.05).
608 609	different superscript letters are significantly different (p<0.05). Figure 6. Acylcarnitine levels in <i>GHR</i> -KO pigs and WT controls. (A) Sum of long-chain
609	Figure 6. Acylcarnitine levels in <i>GHR</i> -KO pigs and WT controls. (A) Sum of long-chain
609 610	Figure 6. Acylcarnitine levels in <i>GHR</i> -KO pigs and WT controls. (A) Sum of long-chain acylcarnitines. (B) Sum of short-chain acylcarnitines. (C)Free carnitine. (D) CPT1 ratio as a
609 610 611	Figure 6. Acylcarnitine levels in <i>GHR</i> -KO pigs and WT controls. (A) Sum of long-chain acylcarnitines. (B) Sum of short-chain acylcarnitines. (C)Free carnitine. (D) CPT1 ratio as a proxy for the activity of carnitine palmitoyltransferase 1A (CPT1A). (E) Ratio of acetylcarnitine
609 610 611 612	Figure 6. Acylcarnitine levels in <i>GHR</i> -KO pigs and WT controls. (A) Sum of long-chain acylcarnitines. (B) Sum of short-chain acylcarnitines. (C)Free carnitine. (D) CPT1 ratio as a proxy for the activity of carnitine palmitoyltransferase 1A (CPT1A). (E) Ratio of acetylcarnitine (C2) and propionylcarnitine (C3) to free carnitine (C0) as a measure for beta-oxidation
609 610 611 612 613	Figure 6. Acylcarnitine levels in <i>GHR</i> -KO pigs and WT controls. (A) Sum of long-chain acylcarnitines. (B) Sum of short-chain acylcarnitines. (C)Free carnitine. (D) CPT1 ratio as a proxy for the activity of carnitine palmitoyltransferase 1A (CPT1A). (E) Ratio of acetylcarnitine (C2) and propionylcarnitine (C3) to free carnitine (C0) as a measure for beta-oxidation activity. The box plots show medians, interquartile range (box) and extremes (whiskers). The
609 610 611 612 613 614	Figure 6. Acylcarnitine levels in <i>GHR</i> -KO pigs and WT controls. (A) Sum of long-chain acylcarnitines. (B) Sum of short-chain acylcarnitines. (C)Free carnitine. (D) CPT1 ratio as a proxy for the activity of carnitine palmitoyltransferase 1A (CPT1A). (E) Ratio of acetylcarnitine (C2) and propionylcarnitine (C3) to free carnitine (C0) as a measure for beta-oxidation activity. The box plots show medians, interquartile range (box) and extremes (whiskers). The mean is marked as "+". Results of analysis of variance are indicated: G: p-value of the effect
609 610 611 612 613 614 615	Figure 6. Acylcarnitine levels in <i>GHR</i> -KO pigs and WT controls. (A) Sum of long-chain acylcarnitines. (B) Sum of short-chain acylcarnitines. (C)Free carnitine. (D) CPT1 ratio as a proxy for the activity of carnitine palmitoyltransferase 1A (CPT1A). (E) Ratio of acetylcarnitine (C2) and propionylcarnitine (C3) to free carnitine (C0) as a measure for beta-oxidation activity. The box plots show medians, interquartile range (box) and extremes (whiskers). The mean is marked as "+". Results of analysis of variance are indicated: G: p-value of the effect of Group; A: p-value of the effect of Age; G*A: p-value of the interaction Group*Age. Means
609 610 611 612 613 614 615 616	Figure 6. Acylcarnitine levels in <i>GHR</i> -KO pigs and WT controls. (A) Sum of long-chain acylcarnitines. (B) Sum of short-chain acylcarnitines. (C)Free carnitine. (D) CPT1 ratio as a proxy for the activity of carnitine palmitoyltransferase 1A (CPT1A). (E) Ratio of acetylcarnitine (C2) and propionylcarnitine (C3) to free carnitine (C0) as a measure for beta-oxidation activity. The box plots show medians, interquartile range (box) and extremes (whiskers). The mean is marked as "+". Results of analysis of variance are indicated: G: p-value of the effect of Group; A: p-value of the effect of Age; G*A: p-value of the interaction Group*Age. Means with different superscript letters are significantly different (p<0.05).

- effect of Group; A: p-value of the effect of Age; G*A: p-value of the interaction Group*Age. 620 Means with different superscript letters are significantly different (p<0.05). 621 622 Figure S1. Glucose (A-C), insulin (D-F) levels and APE (G-I) in control and GHR-KO pigs during HEC. 623 Figure S2. Representative cross-sections of subcutaneous adipose tissue/longissimus 624 625 lumborum muscle at the level of the last rib in a young vs adult wild-type control (top) and young and adult *GHR*-KO pig (bottom). 626 627 Figure S3. Effect of castration at infancy on adult GHR-KO pigs. (A) Fat-to-muscle ratio (thickness of overlaying subcutaneous adipose tissue / longissimus lumborum muscle 628 height). (B) Glucose, (C) Glucose infusion rate (GIR) in intact vs. early castrated GHR-KO 629 pigs at adult age, (D) M-value, (E) NEFA, (F) β-hydroxybutyrate levels. The box plots show 630 median, interquartile range (box) and extremes (whiskers). The mean is marked as "+". 631 Results of analysis of variance are indicated: G: p-value of the effect of Group; S: p-value of 632 633 the effect of Sex. Figure S4. Partial Least Squares Discriminant Analysis (PLS-DA) of targeted metabolomic 634 profiles in young and adult GHR-KO and WT pigs. 635 636 Figure S5. Ratio of unsaturated (UFA) to saturated (SFA) lysophosphatidylcholines (LPCs, A) phosphatidylcholines (PCs, B) in GHR-KO pigs and WT controls. The box plots show 637 median, interquartile range (box) and extremes (whiskers). The mean is marked as "+". 638 Results of analysis of variance are indicated: G: p-value of the effect of Group; A: p-value of 639 the effect of Age; G*A: p-value of the interaction Group*Age. Means with different superscript 640 letters are significantly different (p<0.05). 641 Figure S6. Heat map of the expression pattern of genes involved in lipolysis, adipogenesis 642 643 and lipid desaturation in GHR-KO vs. WT subcutaneous adipose tissue, clustered for genes 644 (A) and groups (B). Effects of analysis of variance are indicated when showing p-value <0.05 645 for Group, Age and/or Group x Age. 646 References 647
- Vijayakumar, A., et al., Biological Effects of Growth Hormone on Carbohydrate and Lipid
 Metabolism. Growth hormone & IGF research: official journal of the Growth Hormone
 Research Society and the International IGF Research Society, 2010. 20(1): p. 1.
- Sharma, R., et al., *Effect of growth hormone on insulin signaling*. Molecular and cellular endocrinology, 2020. **518**: p. 111038.
- Laron, Z., Laron syndrome (primary growth hormone resistance or insensitivity): the personal experience 1958-2003. J Clin Endocrinol Metab, 2004. **89**(3): p. 1031-44.

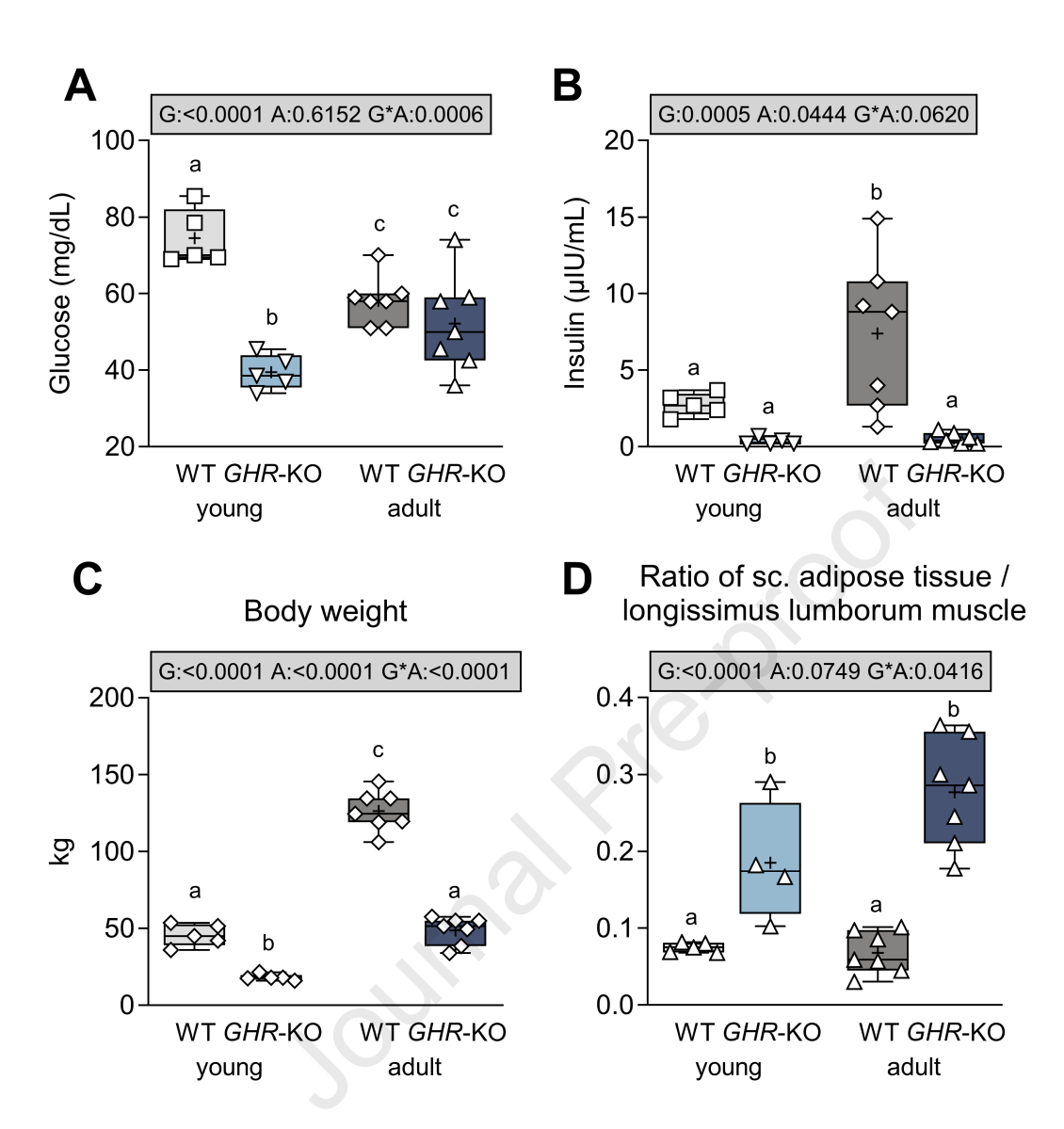
- List, E.O., et al., Endocrine parameters and phenotypes of the growth hormone receptor gene disrupted (GHR-/-) mouse. Endocr Rev, 2011. **32**(3): p. 356-86.
- Guevara-Aguirre, J., et al., GH Receptor Deficiency in Ecuadorian Adults Is Associated With
 Obesity and Enhanced Insulin Sensitivity. The Journal of Clinical Endocrinology & Metabolism,
 2015. 100(7): p. 2589-2596.
- 6. Guevara-Aguirre, J., et al., *Growth hormone receptor deficiency is associated with a major* 661 *reduction in pro-aging signaling, cancer, and diabetes in humans*. Sci Transl Med, 2011. **3**(70): 662 p. 70ra13.
- Husbands, S., et al., *Increased insulin sensitivity in young, growth hormone deficient children.*Clinical Endocrinology, 2001. **55**(1): p. 87-92.
- Rosenfeld, R.G., A.L. Rosenbloom, and J. Guevara-Aguirre, *Growth hormone (GH) insensitivity due to primary GH receptor deficiency.* Endocrine reviews, 1994. **15**(3): p. 369-390.
- Hinrichs, A., et al., MECHANISMS IN ENDOCRINOLOGY: Transient juvenile hypoglycemia in
 growth hormone receptor deficiency—mechanistic insights from Laron syndrome and tailored
 animal models. European Journal of Endocrinology, 2021. 185(2): p. R35-R47.
- 570 10. Zettler, S., et al., A decade of experience with genetically tailored pig models for diabetes and metabolic research. Animal Reproduction, 2020. **17**.
- Hinrichs, A., et al., Growth hormone receptor-deficient pigs resemble the pathophysiology of human Laron syndrome and reveal altered activation of signaling cascades in the liver.
 Molecular metabolism, 2018. 11: p. 113-128.
- Hinrichs, A., et al., *Growth hormone receptor knockout to reduce the size of donor pigs for preclinical xenotransplantation studies.* Xenotransplantation, 2020: p. e12664.
- 577 Schilloks, M.-C., et al., *Effects of GHR Deficiency and Juvenile Hypoglycemia on Immune Cells*678 of a Porcine Model for Laron Syndrome. Biomolecules, 2023. **13**(4): p. 597.
- Shashikadze, B., et al., Structural and proteomic repercussions of growth hormone receptor
 deficiency on the pituitary gland–lessons from a translational pig model. Journal of
 Neuroendocrinology, 2023: p. e13277.
- Young, J.A., et al., *Growth hormone insensitivity and adipose tissue: tissue morphology and transcriptome analyses in pigs and humans.* Pituitary, 2023: p. 1-15.
- Laane, L., et al., Decreased β-cell volume and insulin secretion but preserved glucose
 tolerance in a growth hormone insensitive pig model. Pituitary, 2024: p. 1-10.
- Eckstein, Y., et al., *Protocol for in vivo assessment of glucose control and insulin secretion and sensitivity in the pig.* STAR protocols, 2025. **6**(2): p. 103774.
- Landau, B.R., et al., *Use of 2H2O for estimating rates of gluconeogenesis. Application to the* fasted state. The Journal of clinical investigation, 1995. **95**(1): p. 172-178.
- Jones, J., et al., Simplified analysis of acetaminophen glucuronide for quantifying
 gluconeogenesis and glycogenolysis using deuterated water. Analytical Biochemistry, 2015.
 479: p. 37-39.
- Landau, B.R., et al., *Use of 2H2O for estimating rates of gluconeogenesis. Application to the* fasted state. J Clin Invest, 1995. **95**(1): p. 172-8.
- Bódis, K., et al., Expansion and Impaired Mitochondrial Efficiency of Deep Subcutaneous
 Adipose Tissue in Recent-Onset Type 2 Diabetes. J Clin Endocrinol Metab, 2020. 105(4): p.
 e1331-43.
- 698 22. Szendroedi, J., et al., *Cohort profile: the German diabetes study (GDS).* Cardiovascular diabetology, 2016. **15**: p. 1-14.
- 700 23. Roden, M., *Clinical diabetes research: methods and techniques*. 2007: John Wiley & Sons.
- 701 24. Szendroedi, J., et al., *Abnormal hepatic energy homeostasis in type 2 diabetes.* Hepatology, 2009. **50**(4): p. 1079-1086.
- Sarabhai, T., et al., *Monounsaturated fat rapidly induces hepatic gluconeogenesis and whole-body insulin resistance.* JCI insight, 2020. **5**(10).
- Pafili, K., et al., Mitochondrial respiration is decreased in visceral but not subcutaneous
 adipose tissue in obese individuals with fatty liver disease. Journal of Hepatology, 2022. 77(6):
 p. 1504-1514.

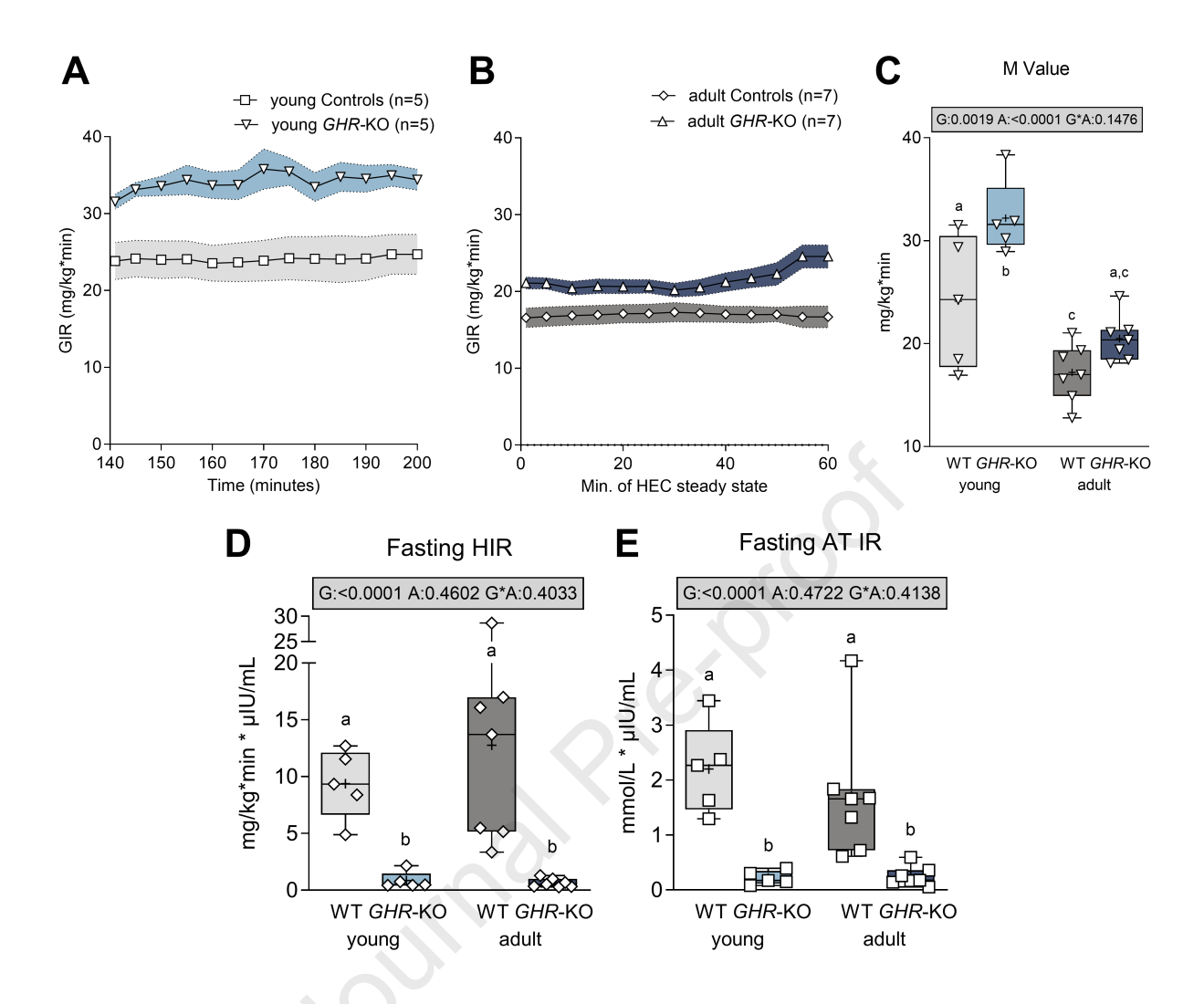
- 708 27. Bidlingmaier, M., et al., Reference intervals for insulin-like growth factor-1 (igf-i) from birth to 709 senescence: results from a multicenter study using a new automated chemiluminescence IGF-I 710 immunoassay conforming to recent international recommendations. The Journal of Clinical 711 Endocrinology & Metabolism, 2014. **99**(5): p. 1712-1721.
- 712 28. Rathkolb, B., et al., *Clinical chemistry and other laboratory tests on mouse plasma or serum.*713 Current protocols in mouse biology, 2013. **3**(2): p. 69-100.
- 714 29. Kunz, S., et al., *Age-and sex-adjusted reference intervals for steroid hormones measured by*715 *liquid chromatography—tandem mass spectrometry using a widely available kit.* Endocrine
 716 Connections, 2024. **13**(1).
- 717 30. Zukunft, S., et al., *High-throughput extraction and quantification method for targeted metabolomics in murine tissues.* Metabolomics, 2018. **14**: p. 1-12.
- 719 31. Pang, Z., et al., *MetaboAnalyst 6.0: towards a unified platform for metabolomics data*720 *processing, analysis and interpretation.* Nucleic acids research, 2024. **52**(W1): p. W398-W406.
- 721 32. Albl, B., et al., *Tissue Sampling Guides for Porcine Biomedical Models*. Toxicol Pathol, 2016.
- 722 33. Schneider, C.A., W.S. Rasband, and K.W. Eliceiri, *NIH Image to ImageJ: 25 years of image analysis*. Nature Methods, 2012. **9**(7): p. 671-675.
- 34. Babicki, S., et al., *Heatmapper: web-enabled heat mapping for all.* Nucleic acids research, 2016. **44**(W1): p. W147-W153.
- 726 35. Kraemer, F.B. and W.-J. Shen, *Hormone-sensitive lipase*. Journal of Lipid Research, 2002.
 727 43(10): p. 1585-1594.
- 728 36. Anthonsen, M.W., et al., *Identification of novel phosphorylation sites in hormone-sensitive*729 *lipase that are phosphorylated in response to isoproterenol and govern activation properties*730 *in vitro.* Journal of Biological Chemistry, 1998. **273**(1): p. 215-221.
- 731 37. Watt, M.J., et al., *Regulation of HSL serine phosphorylation in skeletal muscle and adipose*732 *tissue*. American Journal of Physiology-Endocrinology and Metabolism, 2006. **290**(3): p. E500733 E508.
- 38. Bartlett, K. and S. Eaton, *Mitochondrial β-oxidation*. European Journal of Biochemistry, 2004.
 735 **271**(3): p. 462-469.
- 736 39. Wang, T.J., et al., *Metabolite profiles and the risk of developing diabetes.* Nat Med, 2011. **17**(4): p. 448-53.
- 738 40. Paton, C.M. and J.M. Ntambi, *Biochemical and physiological function of stearoyl-CoA desaturase*. Am J Physiol Endocrinol Metab, 2009. **297**(1): p. E28-37.
- 740 41. Potter, L.R., *Natriuretic peptide metabolism, clearance and degradation.* The FEBS journal, 2011. **278**(11): p. 1808-1817.
- 742 42. Cignarelli, A., et al., *Insulin and Insulin Receptors in Adipose Tissue Development*. Int J Mol Sci, 2019. **20**(3).
- Ravaut, G., et al., *Monounsaturated Fatty Acids in Obesity-Related Inflammation*. Int J Mol Sci, 2020. **22**(1).
- 746 44. Young, J.A., et al., *GHR*-/- *Mice are protected from obesity-related white adipose tissue inflammation.* Journal of neuroendocrinology, 2020. **32**(11): p. e12854.
- 748 45. Møller, N. and J.O.L. Jørgensen, *Effects of Growth Hormone on Glucose, Lipid, and Protein Metabolism in Human Subjects.* Endocrine Reviews, 2009. **30**(2): p. 152-177.
- 750 46. Arlien-Søborg, M.C., et al., *Reversible insulin resistance in muscle and fat unrelated to the metabolic syndrome in patients with acromegaly.* EBioMedicine, 2022. **75**: p. 103763.
- Höybye, C., et al., Contribution of gluconeogenesis and glycogenolysis to hepatic glucose
 production in acromegaly before and after pituitary microsurgery. Hormone and metabolic
 research, 2008. 40(07): p. 498-501.
- 755 48. Kopchick, J.J., et al., *The effects of growth hormone on adipose tissue: old observations, new mechanisms.* Nat Rev Endocrinol, 2020. **16**(3): p. 135-146.
- 757 49. Vlckova, V., et al., *Hypoglycaemia with pioglitazone: analysis of data from the Prescription-*758 *Event Monitoring study.* J Eval Clin Pract, 2010. **16**(6): p. 1124-8.

- Leonard, C.E., et al., Comparative risk of severe hypoglycemia among concomitant users of
 thiazolidinedione antidiabetic agents and antihyperlipidemics. Diabetes Res Clin Pract, 2016.
 115: p. 60-7.
- Salehi, M., et al., *Hypoglycemia After Gastric Bypass Surgery: Current Concepts and Controversies*. J Clin Endocrinol Metab, 2018. 103(8): p. 2815-2826.
- Sprague, J.E. and A.M. Arbeláez, *Glucose counterregulatory responses to hypoglycemia*.
 Pediatric endocrinology reviews : PER, 2011. 9(1): p. 463-475.
- 53. Laron, Z., Y. Avitzur, and B. Klinger, *Carbohydrate metabolism in primary growth hormone* resistance (Laron syndrome) before and during insulin-like growth factor-I treatment.
 Metabolism-Clinical and Experimental, 1995. 44: p. 113-118.
- Riedel, E.O., et al., Functional changes of the liver in the absence of growth hormone (GH)
 action–proteomic and metabolomic insights from a GH receptor deficient pig model.
 Molecular Metabolism, 2020: p. 100978.
- 772 55. Newman, J.C. and E. Verdin, *Ketone bodies as signaling metabolites.* Trends in Endocrinology & Metabolism, 2014. **25**(1): p. 42-52.
- 774 56. Parmar, K., et al., Fasting ketone levels vary by age: implications for differentiating physiologic from pathologic ketotic hypoglycemia. J Pediatr Endocrinol Metab, 2023. **36**(7): p. 667-673.
- 776 57. Hopwood, N.J., et al., *Hypoglycemia in Hypopituitary Children*. American Journal of Diseases of Children, 1975. **129**(8): p. 918-926.
- Ahrén, B. and O. Thorsson, Increased Insulin Sensitivity Is Associated with Reduced Insulin and
 Glucagon Secretion and Increased Insulin Clearance in Man. The Journal of Clinical
 Endocrinology & Metabolism, 2003. 88(3): p. 1264-1270.
- 781 59. McClain, D., et al., *High prevalence of abnormal glucose homeostasis secondary to decreased*782 *insulin secretion in individuals with hereditary haemochromatosis.* Diabetologia, 2006. **49**(7):
 783 p. 1661-1669.
- 784 60. Berryman, D.E., et al., *Comparing adiposity profiles in three mouse models with altered GH signaling.* Growth Hormone & IGF Research, 2004. **14**(4): p. 309-318.
- 786 61. Bennis, M.T., et al., *The role of transplanted visceral fat from the long-lived growth hormone* 787 *receptor knockout mice on insulin signaling.* Geroscience, 2017. **39**: p. 51-59.
- Dominici, F., et al., *Compensatory alterations of insulin signal transduction in liver of growth hormone receptor knockout mice.* Journal of Endocrinology, 2000. **166**(3): p. 579-590.
- 790 63. Sancar, G. and A.L. Birkenfeld, *The role of adipose tissue dysfunction in hepatic insulin* 791 *resistance and T2D.* J Endocrinol, 2024. **262**(3).
- 792 64. Samuel, Varman T. and Gerald I. Shulman, *Mechanisms for Insulin Resistance: Common Threads and Missing Links*. Cell, 2012. **148**(5): p. 852-871.
- 794 65. Roden, M. and G.I. Shulman, *The integrative biology of type 2 diabetes*. Nature, 2019. **576**(7785): p. 51-60.
- Nellemann, B., et al., *Growth hormone-induced insulin resistance in human subjects involves* reduced pyruvate dehydrogenase activity. Acta physiologica, 2014. **210**(2): p. 392-402.
- 798 67. Randle, P., et al., *The glucose fatty-acid cycle its role in insulin sensitivity and the metabolic disturbances of diabetes mellitus.* The Lancet, 1963. **281**(7285): p. 785-789.
- 800 68. Laron, Z., *Hypoglycemia due to hormone deficiencies*. Journal of Pediatric Endocrinology and Metabolism, 1998. **11**(Supplement): p. 117-120.
- 802 69. Jang, C., et al., *Metabolite exchange between mammalian organs quantified in pigs*. Cell metabolism, 2019. **30**(3): p. 594-606. e3.

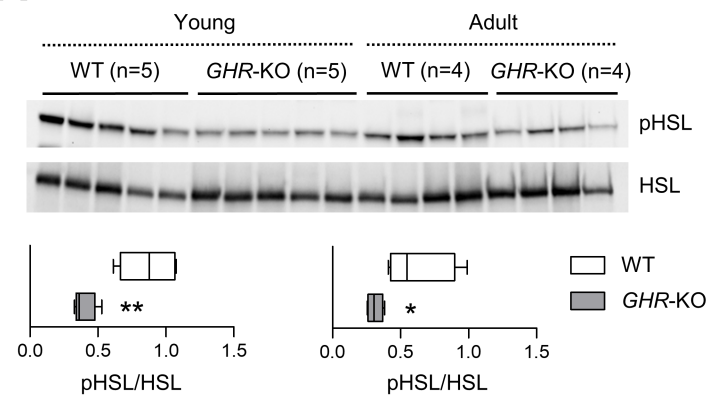
Parameter	young WT	young <i>GHR</i> -KO	adult WT	adult <i>GHR</i> -KO	Group	Age	Group*Age
IGF1 (ng/mL)	344.1±21.0	17.0±21.0	202.1±17.8	19.5±20.2	<0.0001	0.0051	0.0039
Body weight (kg)	45.6±4.2	18.2±4.2	126.2±3.6	48.7±3.5	<0.0001	<0.0001	<0.0001
subcutaneous fat (cm)	0.4±0.02	0.5±0.1	0.5±0.07	1.2±0.1	0.0004	0.0022	0.0160
Muscle (m. long. lumb.) (cm)	5.1±0.3	3.0±0.3	6.9±0.08	4.2±0.2	<0.0001	<0.0001	0.2372
Fat / muscle ratio	0.07±0.003	0.19±0.04	0.07±0.01	0.28±0.02	<0.0001	0.0749	0.0416

Table 1. GH insensitivity related alterations in body composition of *GHR*-KO vs. WT pigs. Mean ± SEM; results of analysis of variance.

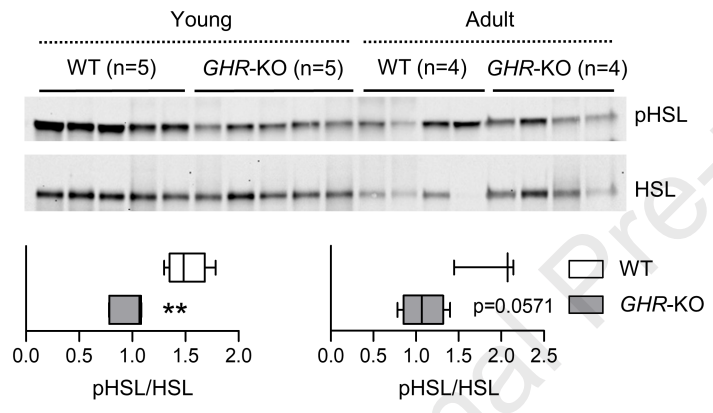


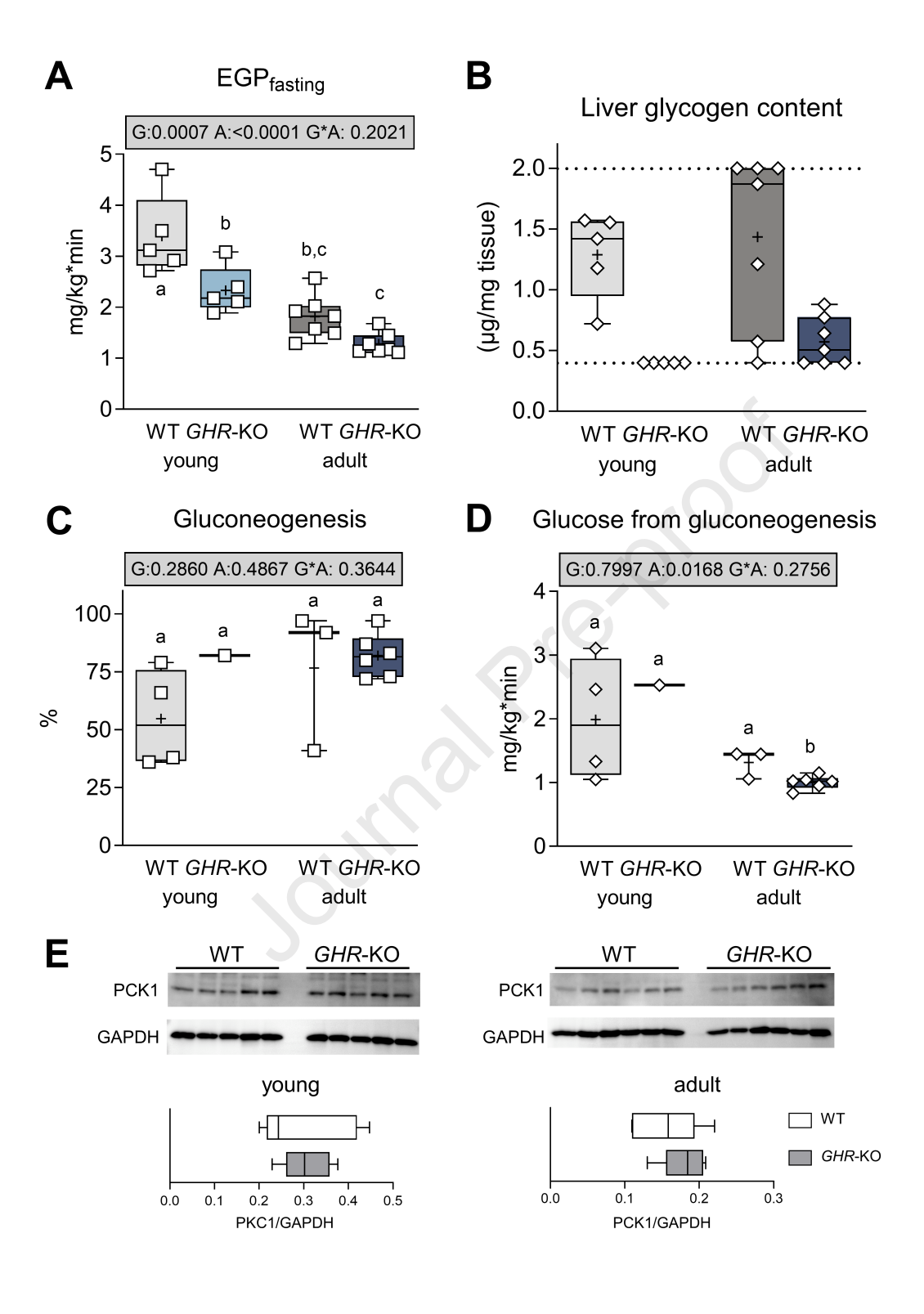


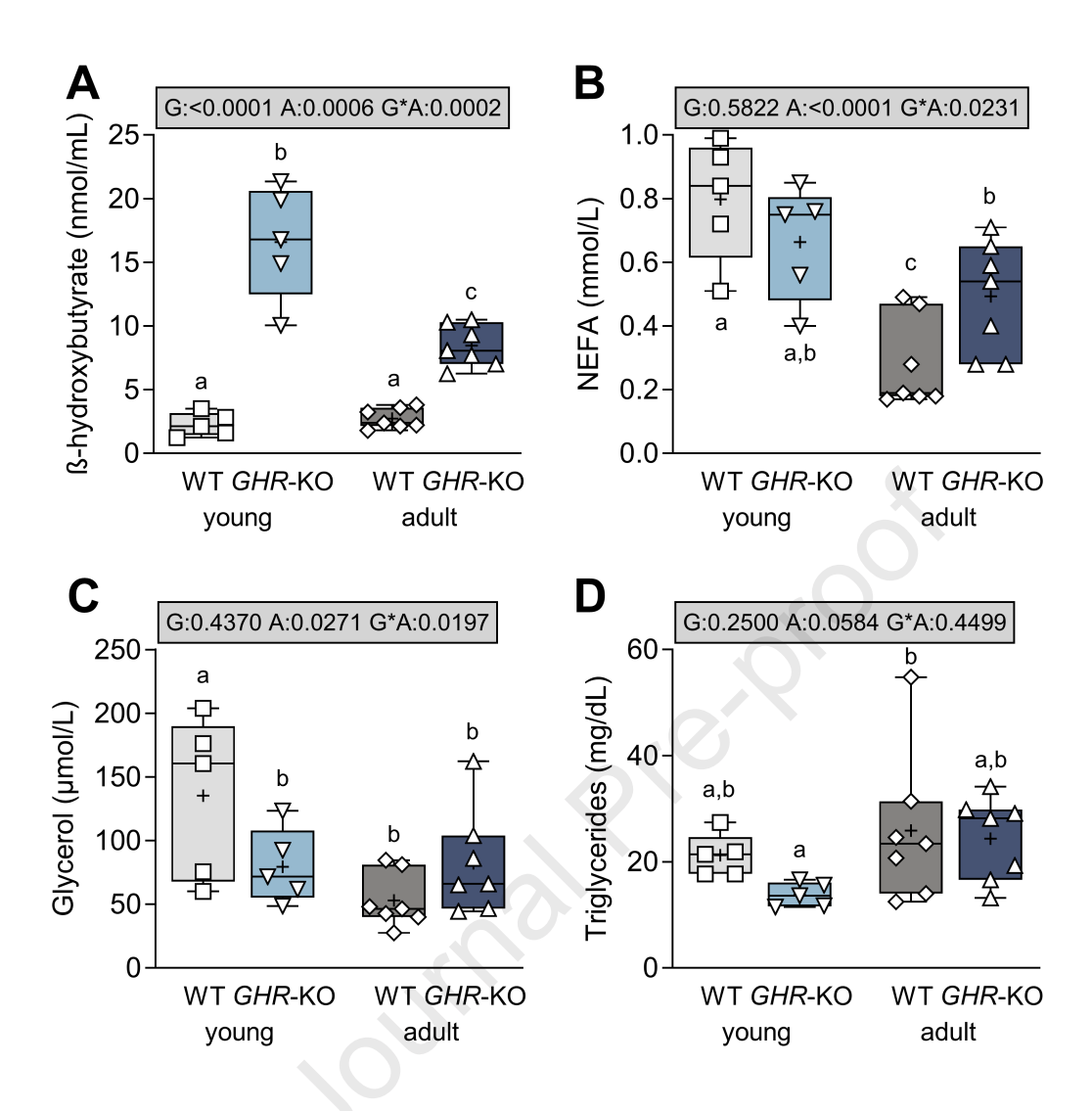
A subcutaneous adipose tissue

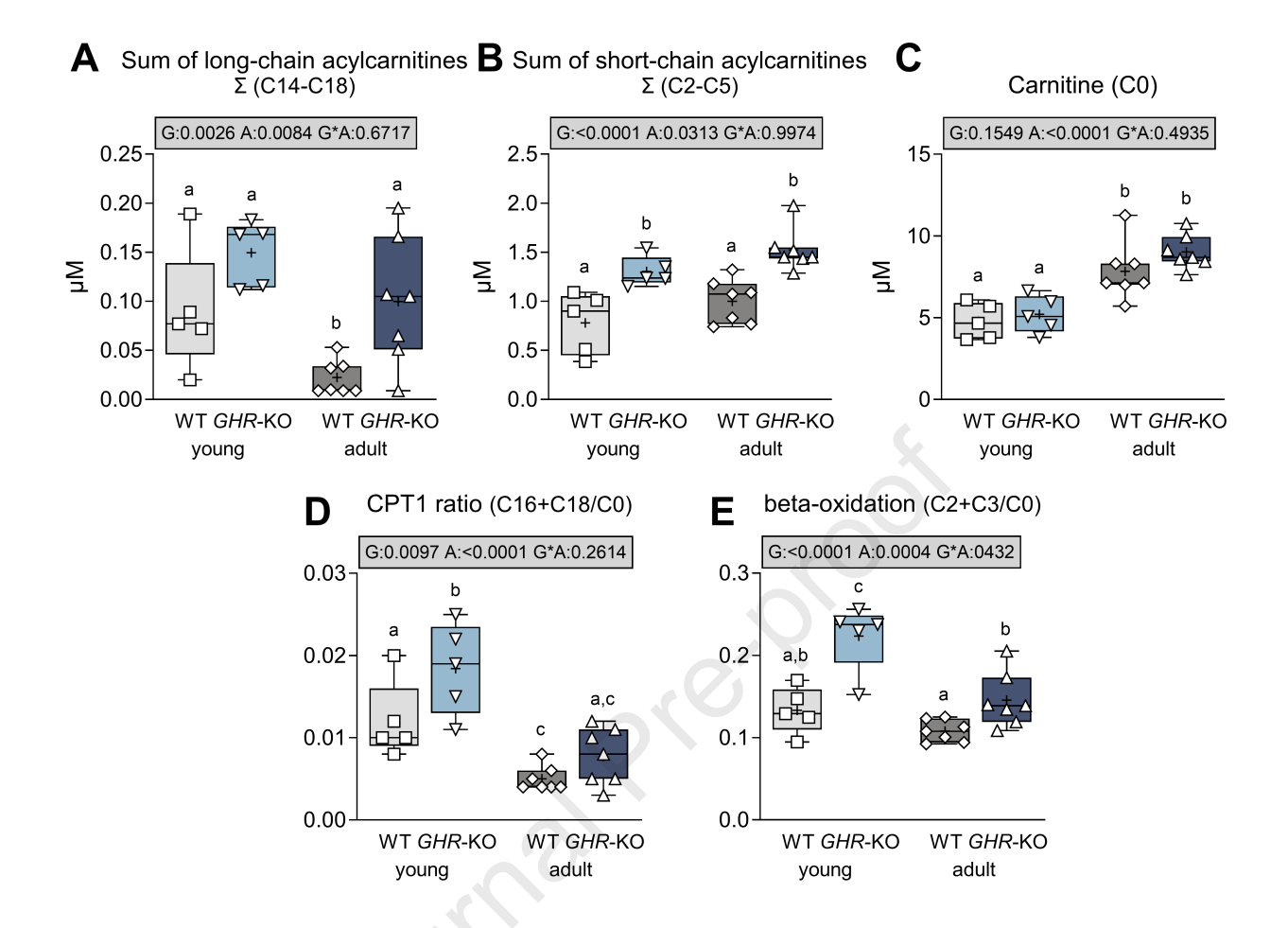


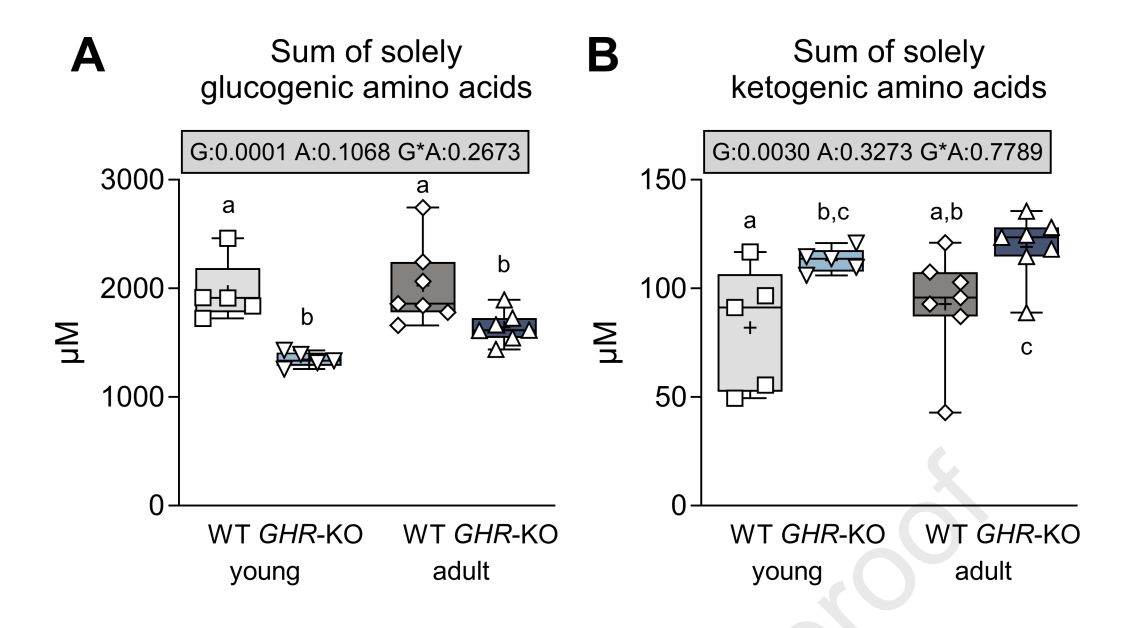
B visceral adipose tissue

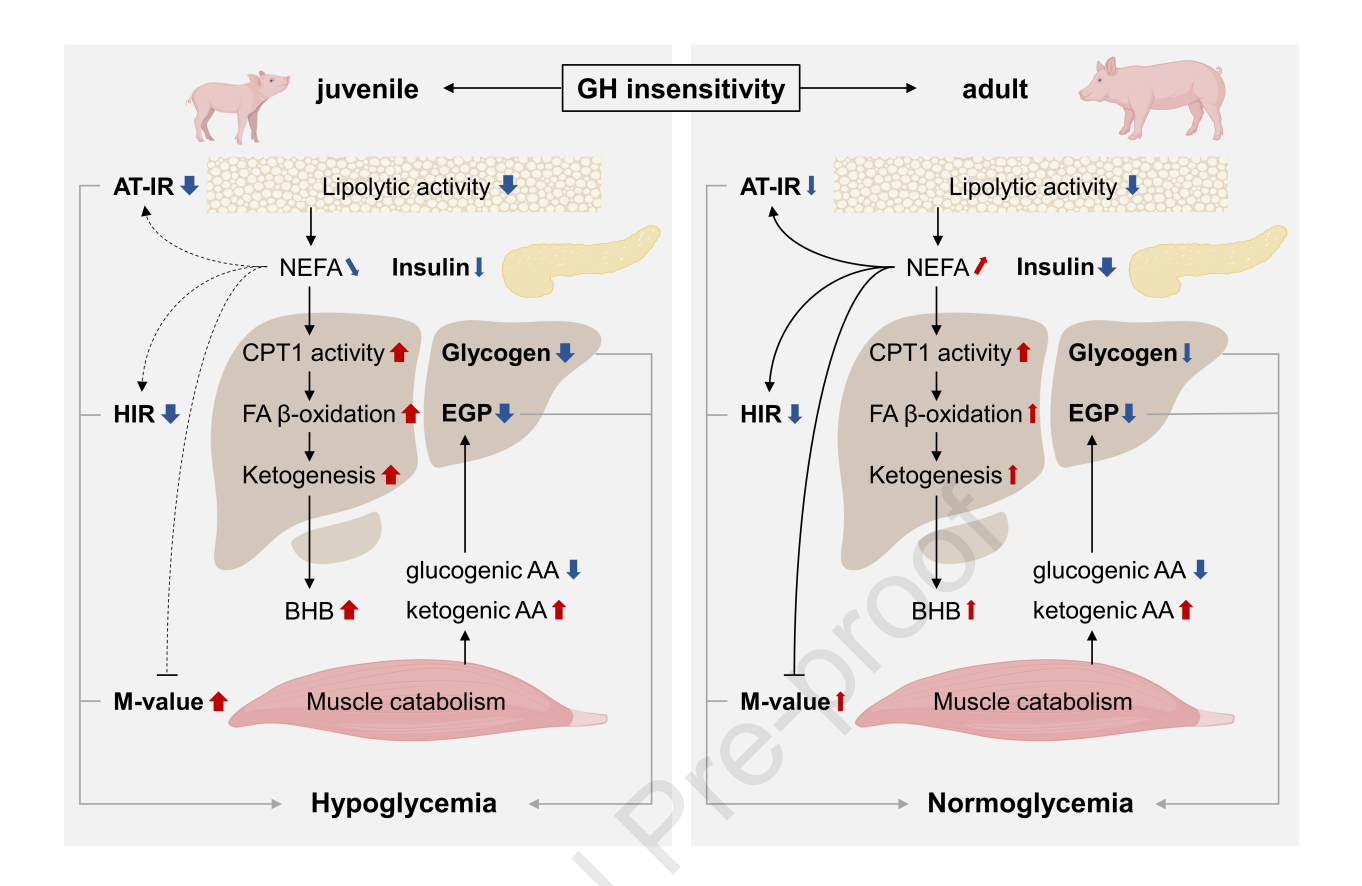












Highlights:

- GHR-KO pigs show transient juvenile hypoglycemia, resembling human Laron syndrome
- Young GHR-KO pigs display insulin hypersensitivity, reduced EGP, increased betaoxidation and ketosis
- Adult GHR-KO pigs accumulate adipose tissue, are less insulin sensitive and normoglycemic
- The transition to normoglycemia does not depend on sex hormones

The authors declare no competing interest regarding the work in the manuscript entitled "Insulin sensitivity—driven juvenile hypoglycemia in GH insensitivity: Age-dependent metabolic adaptations in a porcine model for Laron syndrome".